

## Transport of magnetic turbulence in SNR

---

**R. Brose\***, I. Telezhinsky, M. Pohl

*Institute of Physics and Astronomy, University of Potsdam, Karl-Liebknecht-Str. 24/25, 14476  
Potsdam, Germany*

*DESY, Platanenallee 6, 15738 Zeuthen, Germany*

*E-mail: [robert.brose@desy.de](mailto:robert.brose@desy.de)*

Supernova remnants are known as sources of galactic cosmic rays for their non-thermal emission of radio waves, X-rays, and gamma-rays. However, the observed soft broken power-law spectra are hard to reproduce within standard acceleration theory based on the assumption of Bohm diffusion. Here we model cosmic ray acceleration in a time-dependent and self-consistent way by simultaneous solving the coupled transport equations for cosmic rays and isotropic scattering turbulence. The transport equation for cosmic ray is solved in a test-particle approach while the equation for scattering turbulence considers just Alfvén waves. Their spectral energy density determines the spatial diffusion coefficient of cosmic rays. Our co-moving expanding grid extends upstream to several shock radii, so we are able to self-consistently study the escape of CRs from their acceleration site. We demonstrate that the system is typically not in a steady state. In fact, even after several thousand years of evolution, no equilibrium situation is reached. The resulting time-dependent particle spectra obtained in this work strongly differ from those derived assuming a steady state and Bohm diffusion. Our results indicate that the proper account for the evolution of scattering turbulence and hence particle diffusion coefficient is crucial for the formation of the observed soft spectra and spectral breaks.

*The 34th International Cosmic Ray Conference,  
30 July- 6 August, 2015  
The Hague, The Netherlands*

---

\*Speaker.

## 1. Introduction

Diffusive shock acceleration (DSA) at the forward shock of a Supernova remnant (SNR) is an efficient process that relies on self-generated turbulence [1]. Streaming cosmic rays (CRs) in the upstream region of the shock generate magnetic turbulence that enhances the acceleration process, which in turn leads to further turbulence growth. This process is terminated by escape of CRs or generally when the growth time of turbulence becomes longer than the evolutionary time scale of the system. Conventionally, it is considered that turbulence growth is the fastest process in the system, which is then followed by particle acceleration, and finally by global magneto-hydrodynamical (MHD) evolution of the SNR. It is then often assumed that for the first two processes a quasi-equilibrium develops which slowly changes on account of the MHD evolution. Under the assumption of steady state for both turbulence and particle transport, the cosmic ray distribution at the shock can be derived accounting for their feedback [2, 3]. It can then be imposed on global SNR models [4], or, alternatively, one can solve the entire coupled system of turbulence, CRs, and SNR fluid under steady-state conditions and in a very limited shock precursor region [5]. It has been realized, however, that limited time is available as for turbulence growth so for particle acceleration at SNR [6, 7, 8], and so the steady-state assumption for turbulence and CRs up to the highest energies is questionable.

Here, we introduce a fully time-dependent calculation of the cosmic ray acceleration coupled to the evolution of isotropic Alfvénic turbulence using the analytical self-similar description for SNR parameters. Our model self-consistently describes and realistically accounts for competing plasma processes. As a result we obtain magnetic turbulence energy density and particle spectra that implicitly include escaping CRs.

## 2. Particle acceleration

To model cosmic ray acceleration we use a kinetic approach in test-particle approximation [9, 10, 11]. We numerically solve the time-dependent transport equation for the differential number density of cosmic rays in spherically-symmetric geometry [12]:

$$\frac{\partial N}{\partial t} = \nabla(D_r \nabla N - \mathbf{u}N) - \frac{\partial}{\partial p} \left( (N\dot{p}) - \frac{\nabla \mathbf{u}}{3} Np \right) + Q \quad (2.1)$$

where  $N$  is the differential number density of cosmic rays,  $D_r$  is the spatial diffusion coefficient,  $\mathbf{u}$  is the advective velocity,  $\dot{p}$  are the energy losses, and  $Q$  is the source of thermal particles that is treated according to the thermal-leakage injection model [13]. The equation is transformed to a frame co-moving with the shock,  $(x-1) = (x^*-1)^3$ , where  $x = r/R_{sh}$  is the radial coordinate normalized to the shock radius. As can be seen, for equidistant binning in  $x^*$  this transformation guarantees a very good resolution close to the shock while simultaneously extending out to several tens of shock radii in the upstream region allowing for keeping all injected particles in the simulation domain.

One of the crucial parameters is the choice of the spatial diffusion coefficient [10]. It governs the efficiency of cosmic-ray acceleration and thus the maximum energy reached by the cosmic rays. It is also responsible for the spatial distribution of accelerated particles both upstream and downstream of the shock, that in turn impacts the subsequent emission from the source and its

vicinity. The diffusion coefficient is usually assumed to be Bohm-like, i.e.,  $D_r = cr_g/3$ ,  $r_g$  being the gyro-radius of the CR. The following arguments suggest that this approach is oversimplified. The diffusion coefficient is directly connected to the magnetic field fluctuations. Let us assume that CRs are being scattered by Alfvén waves that satisfy the resonance condition

$$k = \frac{qB_0}{pc}, \quad (2.2)$$

where  $k$  is the wavenumber,  $q$  is the particle charge, and  $B_0$  is the background magnetic field. The Bohm-diffusion approach is then equivalent to a featureless flat magnetic turbulence spectrum [14, 1]

$$D_r = \frac{4v}{3\pi} r_g \frac{B_0^2}{E_w} \quad (2.3)$$

where  $E_w$  denotes the energy density per unit logarithmic bandwidth of Alfvén waves resonant with particles of momentum  $p$ . If the turbulence is a result of the growth of Alfvén waves (for instance due to resonant amplification by streaming CRs) as well as their spatial transport, compression at the shock, damping by various mechanisms, and spectral energy transfer due to cascading, it is obviously very unlikely that the turbulence spectrum in the SNR and its vicinity is featureless. Besides, from  $\gamma$ -ray observations of SNRs and their surroundings we now understand that i) it is hard to accommodate Bohm diffusion for particles in an energy band as wide as we see in SNRs, and ii) the diffusion around SNRs is much slower than the average Galactic one. Therefore, a more sophisticated approach to calculation of the self-consistent diffusion coefficient is needed [15]. This can be done via calculation of magnetic turbulence spectrum, including all the above processes. This should result in a more realistic and self-consistent picture of cosmic ray acceleration in SNRs.

### 3. Magnetic turbulence

We consider Alfvén waves as scattering centers for the CRs. Alfvén waves can be considered as a small contribution to the magnetic field at some position, so that  $B_{\text{tot}} = B_0 + \delta b$ , where  $\delta b$  is the amplitude of all waves present at the given position. Averaging the energy density over sufficiently large times gives  $B_{\text{tot}}^2 = B_0^2 + \langle \delta b^2 \rangle$ . The total energy density in the waves can be represented as  $\int E_w(k) d \ln k = \langle \delta b^2 \rangle$ , where  $E_w$  is the magnetic turbulence spectrum in  $k$ -space. The diffusion coefficient can be then calculated using expression (2.3). It allows us to derive the diffusion coefficient of a particle with momentum  $p$  moving in the background field  $B_0$  at any given position.

We consider 1-D spherical-symmetric geometry and treat the turbulence as isotropic. To investigate the growth, damping, cascading, and propagation of the Alfvén waves along the background magnetic field, we have to solve an equation for the transport of the magnetic turbulence along with the transport equation (2.1) for cosmic rays. The transport of magnetic turbulence can be described by the following advection-diffusion equation for the spectral energy density of the waves,  $E_w$ :

$$\frac{\partial E_w}{\partial t} + \mathbf{u} \cdot (\nabla_r E_w) + c_{\text{comp}} (\nabla_r \cdot \mathbf{u}) E_w + k \frac{\partial}{\partial k} D_k \frac{\partial E_w}{\partial k} \frac{1}{k^3} = 2(\Gamma_g - \Gamma_d) E_w + Q. \quad (3.1)$$

where  $c_{\text{comp}}=1.5$  denotes the pre-factor for the wave compression at the shock,  $D_k$  is the diffusion coefficient in wavenumber space representing cascading,  $\Gamma_g$  and  $\Gamma_d$  are the growth and the damping

rates respectively, and  $Q$  is the injection source for the turbulence. Therefore, we consider growth, damping, advection, compression of turbulence at the shock, as well as spectral energy transfer through cascading in our approach. The magnetic turbulence transport equation (3.1) is transformed to the shock co-moving frame as well as spatially in the same manner as the cosmic-ray transport equation (2.1) leading to the system of two equations solved simultaneously.

Wave growth is at first only considered by resonant amplification of Alfvén waves although the possibility to handle any other growth mechanism exists. The growth rate due to resonant amplification is given by [12, 14]

$$\Gamma_g = \frac{v_A p^2 v}{3E_w} \left| \frac{\partial N}{\partial r} \right|, \quad (3.2)$$

where the growth is driven by the cosmic-ray pressure gradient.

For wave damping we consider neutral-charged collisions and Ion-Cyclotron damping. The damping rate due to neutral-charged collisions is  $\Gamma_{d,nc} = \frac{1}{2} n_H \langle v\sigma \rangle$  [14, 16], where  $n_H$  is the number density of neutral hydrogen and  $\langle v\sigma \rangle$  is the fractional rate of change of the velocity of protons averaged over the velocity distribution. Normally, neutral-charged damping is relatively weak and independent of the wavenumber of Alfvén waves. This mechanism is mostly important in regions of low temperatures and high densities, like in molecular clouds. Cosmic rays may penetrate the clouds where as noted before [17] their spectrum may be strongly modified. Ion-Cyclotron damping is due to interaction of Alfvén waves with the thermal particles of the plasma and is the strongest on small scales  $\Gamma_{d,IC} = \frac{v_A k^2}{2\omega_p}$ , where  $\omega_p$  is the ion plasma frequency [18]. This damping should transfer energy to the plasma via heating, which is not yet considered in this work, though we are aware that it might modify the spectrum around the particles injection scale.

Following [19], cascading is treated as a diffusion process in wavenumber space. Given assumption of isotropic turbulence, the corresponding diffusion coefficient is  $D_k = k^5 v_A \sqrt{\frac{E_w}{2B_0^2}}$ . If cascading is the dominant process, this coefficient will result in Kolmogorov-like turbulence spectrum,  $E_w \propto k^{-2/3}$ .

One should note that in the absence of initial turbulence there is nothing to grow, so Eq. (3.1) requires a seed. We therefore take as an initial condition an ISM turbulence derived with Eq. (2.3) from the diffusion coefficient,  $D_r = 10^{27} \left( \frac{pc}{10 \text{ GeV}} \right)^{1/3} \left( \frac{B_0}{3 \mu\text{G}} \right)^{-1/3}$ . This value of  $D_r$  is a factor of 100 lower than that in the ISM. This choice saves computational time in the initial stages of our simulations and at the same time does not affect the maximum level or strength of the turbulence energy density that we obtain.

#### 4. Evolution of the SNR

We consider the SNR in Sedov-Taylor stage of evolution applicable to the remnants where the impact of the free expansion phase is small on account of its short duration (as in a typical type-Ia SNR). We use analytic approximations to Sedov-Taylor solutions [20] to describe the evolution of the plasma flow parameters. The self-similar solutions for the magnetic field profiles inside the SNR in Sedov-Taylor stage are taken from [21].

## 5. Results

Using the method described above we explored the evolution of the magnetic turbulence spectra along with corresponding particle spectra in the SNRs up to the age of 12000 years. We compare our results obtained from self-consistent calculations with the previously used approach that assumes Bohm diffusion everywhere downstream of the shock with exponential transition to the Galactic diffusion on the scale of one SNR radius ahead of the shock [10, 11]. To guarantee that the cosmic-ray pressure does not violate the test-particle approximation, we tune the injection of thermal particles so that the cosmic-ray pressure stays always below 10% of the ram pressure, and we use the same injection parameters in both calculations.

### 5.1 Turbulence spectra

The evolution of magnetic turbulence spectra at the SNR shock is given at Fig. 1 (left). The turbulence spectra at the shock exhibit a complicated shape. Namely, they have a very extended region of efficient growth that spans several orders of magnitude in  $k$ -space. It is not surprising, because at the position of the shock the turbulence is driven by particles of all energies, and since rather low-energy particles dominate the particle spectrum, the growth of turbulence is fastest at higher  $k$ . However, at some point cascading starts playing a crucial role, and dominates over the growth. This is where a transition to the inertial range happens, and one can see a break in the spectrum. Finally, at higher  $k$ , a classical Kolmogorov power-law turbulence spectrum is observed. Note, an interesting result of such an interplay between growth and cascading is that in a rather wide range of  $k$ -numbers the turbulence spectrum shape appears to be a plateau-like and similar to that of Bohm-diffusion.

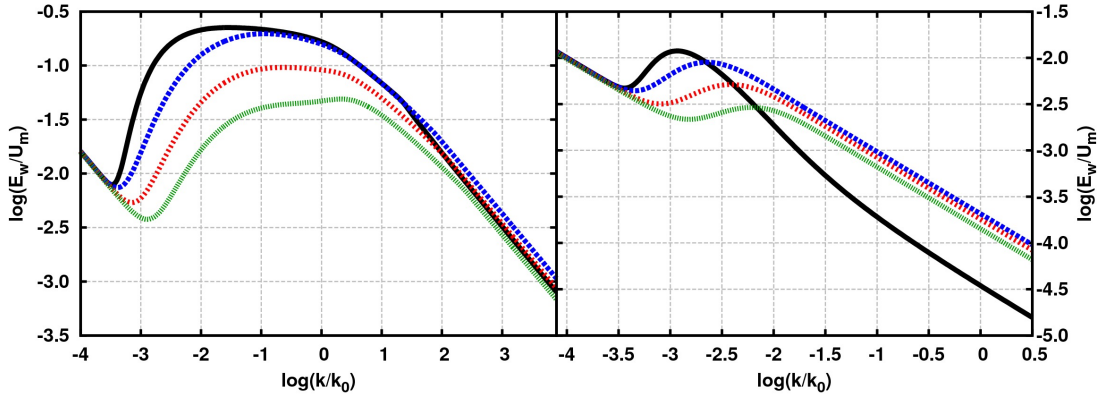


**Figure 1:** Left: Turbulence spectra,  $E_w$ , at the forward shock of the SNR at the age of 200 (black), 2000 (blue), 5000 (red) and 12000 (green) years. Right:  $E_w$  at the distance  $r = 1.15 \cdot R_{shock}$  for the same times.

This interpretation is well supported by the shape of the spectrum further upstream. As we can see from the turbulence spectrum at the shock, particles in a wide energy band should be rather well confined to the shock. However, at low  $k$ -numbers there is a cutoff in the turbulence spectrum, and thus particles beyond some energy can freely escape the shock region. Therefore, at some distance from the shock in the upstream region, one expects to see a particle distribution

that is peaked at around the escape energy. This particle distribution should drive the turbulence there and would correspond to a very narrow  $k$ -region in the turbulence spectrum. For instance, at the position corresponding to 15% of the SNR radius ahead of the shock, there are too few low-energy particles to substantially impact on the turbulence growth, whereas high-energy cosmic rays can easily diffuse further away from the shock. So the turbulence spectrum looks like a classical one (Fig. 1, right): we observe just two regions – the first is the injection region peaked at the wavenumber of maximum growth corresponding to the peak in particle energy spectrum, and the second is a cascading-dominated region at higher wavenumbers. The damping range, that would be the third region of the classical turbulence spectrum, is not shown at Fig. 1 because it is in a region of very high  $k$ -numbers, and is not important in this work.

Note, both plots show that there is no steady state reached during our simulation. The spectral shape at both positions is changing over the whole simulation time, and so does the maximum level of turbulence.

## 5.2 Particle spectra

We compare particle spectra obtained in the self-consistent coupled treatment of magnetic turbulence and cosmic rays to our previous results based on assumption of Bohm diffusion. The downstream volume-integrated spectra are shown at Fig. 2 (left).

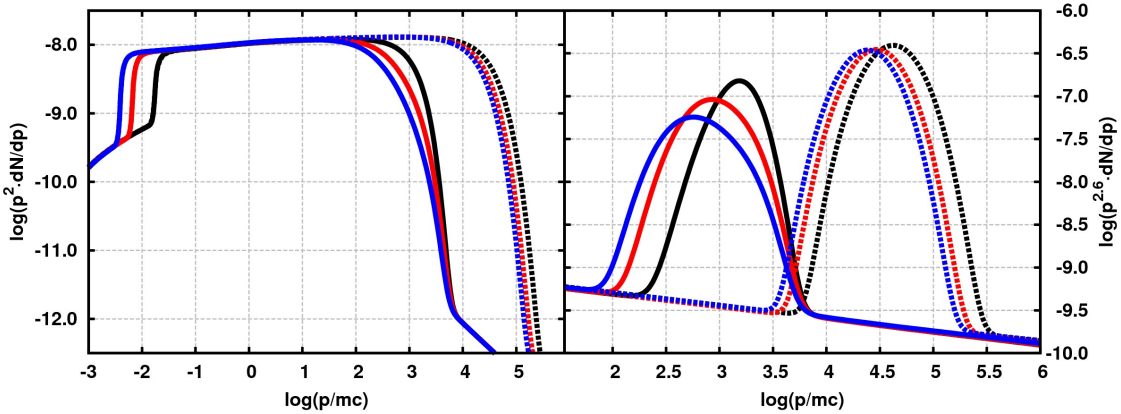


**Figure 2:** Left: the volume-integrated downstream CR spectra for the SNR with the age of 1000 (black), 5000 (red) and 12000 (blue) years. Right: the volume-integrated spectra in a shell of 0.5 pc in diameter at  $r = 1.15 \cdot R_{shock}$  for the same times shows. Solid lines are the results for the self-consistent treatment and dashed lines for the Bohm-like diffusion.

Both calculations show similar power-law spectra, however, with different cutoff regions. In the case of Bohm diffusion, a classical exponential cutoff happens at very high (for the assumed magnetic field) energies. On the other hand, the self-consistent calculation shows systematically lower maximum energies and a less smooth cutoff that is softer than exponential. Moreover, there is a trend of spectral softening in the cutoff region with time. This happens because the turbulence amplitude changes with time. In particular, it drops and allows a more effective particle escape. Escape becomes possible at lower particle energies than for a constant turbulence amplitude. On account of decreasing turbulence, the maximum particle energy also drops faster with time than in

the Bohm-diffusion approximation. The evolution of the CR maximum energy and particle escape history is most prominent in the escaped particle distribution. In particular, it is interesting to consider a particle population in a shell upstream at some distance from the shock. Ahead of the shock it is expected that particle distribution is dominated by escaping particles. For Bohm diffusion this is a log-parabola [22] centered around maximum energy, exactly what we observe at Fig. 2 (right). Instead, our coupled calculation shows shapes evolving with time (Fig. 2, right). Only at the very beginning when the turbulence is sufficiently high, the shape resembles a log-parabola. Later on, as the turbulence amplitude drops, the escaped-particle distribution shifts to lower energies and becomes substantially broader. Exactly this results in a softening and broadening of the cutoff region of the downstream particle distribution, which under certain conditions can be fitted with a broken power-law and cutoff.

In general, the self-consistent treatment introduces a connection between the maximum energy and the injection parameter. To reach higher energies more particles have to be injected because the growth rate (3.2) is proportional to the gradient of the CR-distribution (at least for the resonant instability). This gradient determines the maximum level of turbulence which defines the cutoff energy. In fact, such a dependence to some extent eliminates the magnetic-field strength as the parameter defining the cutoff energy. Furthermore, the injection parameter is no longer an arbitrary parameter that simply scales the CR number density that is directly connected to the observed photon fluxes, but may be constrained by both intensity and cutoff energy in observational data.

## 6. Conclusions

We developed a model for particle acceleration in SNR by solving the time-dependent transport equations for magnetic turbulence and cosmic rays respectively. Our approach is 1-D and limited to the test-particle regime. We consider the cosmic rays being scattered by isotropic, Alfvénic turbulence that is subject to compression, advection, cascading, damping and growth due to resonant amplification of Alfvén waves.

We found that even for old remnants there is no steady state reached. Even after more than 10000 years both turbulence and particle spectra are still evolving. Enhanced escape in the self-consistent treatment gives rise to the formation of spectral breaks and softer spectra at late stages of the SNR evolution similar to those observed in high-energy gamma-rays. The maximum energy of cosmic rays tends to be lower than is estimated in earlier steady state models.

We acknowledge support by the Helmholtz Alliance for Astroparticle Physics HAP funded by the Initiative and Networking Fund of the Helmholtz Association.

## References

- [1] R. Blandford and D. Eichler.
- [2] P. Blasi.
- [3] D. Caprioli, P. Blasi, E. Amato, and M. Vietri.



- [4] D. C. Ellison, P. Slane, D. J. Patnaude, and A. M. Bykov.
- [5] A. M. Bykov, D. C. Ellison, S. M. Osipov, and A. E. Vladimirov.
- [6] P. O. Lagage and C. J. Cesarsky.
- [7] A. R. Bell, K. M. Schure, B. Reville, and G. Giacinti.
- [8] K. M. Schure and A. R. Bell. Cosmic ray acceleration in young supernova remnants. *MNRAS*, 435:1174–1185, October 2013.
- [9] I. Telezhinsky, V. V. Dwarkadas, and M. Pohl. *Astroparticle Physics*, 35:300–311, January 2012.
- [10] I. Telezhinsky, V. V. Dwarkadas, and M. Pohl. *A&A*, 541:A153, May 2012.
- [11] I. Telezhinsky, V. Dwarkadas, and M. Pohl. In *AAS/High Energy Astrophysics Division*, volume 13 of *AAS/High Energy Astrophysics Division*, page 127.16, April 2013.
- [12] J. Skilling. *MNRAS*, 172:557–566, September 1975.
- [13] S. Gabici, P. Blasi, and G. Vannoni. In T. Bulik, B. Rudak, and G. Madejski, editors, *Astrophysical Sources of High Energy Particles and Radiation*, volume 801 of *American Institute of Physics Conference Series*, pages 369–372, November 2005.
- [14] A. R. Bell. *MNRAS*, 182:147–156, January 1978.
- [15] H. Yan, A. Lazarian, and R. Schlickeiser. *APJ*, 745:140, February 2012.
- [16] R. M. Kulsrud and C. J. Cesarsky. *ApJ Let.*, 8:189, March 1971.
- [17] M. A. Malkov, P. H. Diamond, and R. Z. Sagdeev. *Nature Communications*, 2:194, February 2011.
- [18] J. Threlfall, K. G. McClements, and I. De Moortel. *A&A*, 525:A155, January 2011.
- [19] R. Schlickeiser.
- [20] D. P. Cox and J. Franco.
- [21] V. P. Korobeinikov.
- [22] D. C. Ellison and A. M. Bykov. *APJ*, 731:87, April 2011.